Structure of self-assembled liposome-DNA-metal complexes

O. Francescangeli, V. Stanic, and L. Gobbi
Dipartimento di Fisica e Ingegneria dei Materiali e del Territorio and Istituto Nazionale per la Fisica della Materia, Università di Ancona, Via Brecce Bianche, 60131 Ancona, Italy

P. Bruni, M. Iacussi, and G. Tosi
Dipartimento di Scienze dei Materiali e della Terra, Università di Ancona, Via Brecce Bianche, 60131 Ancona, Italy

S. Bernstorff
Sincrotrone Trieste, 34012 Basovizza, Trieste, Italy

(Received 24 May 2002; revised manuscript received 30 August 2002; published 16 January 2003)

We have studied the structural and morphological properties of the triple complex dioleoyl phosphatidylcholine (DOPC)-DNA-Mn^{2+} by means of synchrotron x-ray diffraction and freeze-fracture transmission electron microscopy. This complex is formed in a self-assembled manner when water solutions of neutral lipid, DNA, and metal ions are mixed, which represents a striking example of supramolecular chemistry. The DNA condensation in the complex is promoted by the metal cations that bind the polar heads of the lipid with the negatively charged phosphate groups of DNA. The complex is rather heterogeneous with respect to size and shape and exhibits the lamellar symmetry of the L_α^c phase: the structure consists of an ordered multilamellar assembly similar to that recently found in cationic liposome-DNA complexes, where the hydrated DNA helices are sandwiched between the liposome bilayers. The experimental results show that, at equilibrium, globules of the triple complex in the L_α^c phase coexist with globules of multilamellar vesicles of DOPC in the L_α phase, the volume ratio of the two structures being dependent on the molar ratio of the three components DOPC, DNA, and Mn^{2+}. These complexes are of potential interest for applications as synthetically based nonviral carriers of DNA vectors for gene therapy.

DOI: 10.1103/PhysRevE.67.011904 PACS number(s): 87.16.Dg, 87.15.By, 61.30.Eb, 87.14.Cc

I. INTRODUCTION

Accurate characterization of the structure of biomembranes is a major interest of the biophysical community [1]. This characterization includes the lipid bilayer that forms the basic matrix of the membrane as well as the intrinsic proteins which are responsible for most of the biochemical functionality of membranes. On the other hand, the elastic and charge properties of the structurally well-defined DNA macromolecule have led to many important experimental studies in recent years [2].

Liposomes (L) are self-closed structures composed of curved lipid bilayers which entrap part of the solvent, in which they freely float, into the interior [3]. They may consist of one or several concentric membranes and their size ranges from about 20 to several tenths nanometers. The association between neutral liposomes and DNA has been an object of several investigations [4–6] over the past two decades. However, due to extreme weakness of the interactions, the claimed formation of binary complexes do not seem to offer any practical application. On the contrary, cationic liposomes (CLs) complexed with DNA have been shown to be promising nonviral delivery systems for gene therapy applications [7–10]. This is because they are able to mimic certain characteristics of natural viruses in their ability to act as efficient chemical carriers of extracellular DNA across outer cell membranes and nuclear membranes (transfection) [11,12]. The use of nonviral rather than viral methods for gene delivery has several advantages, including nonimmunicity and the potential for transferring and expressing (transfecting) large pieces of DNA into cells. The lower transfection efficiencies of nonviral delivery methods may be improved through insights into transfection-related mechanisms at the molecular and self-assembled levels. For these reasons, in recent years there has been a tremendous surge in interest in elucidating the structures of CL-DNA complexes.

The solution structure of CL-DNA complexes was probed on length scale from subnanometer to micrometer by synchrotron x-ray diffraction (XRD), optical microscopy and freeze-fracture electron microscopy (EM) [10,13–18]. Three different types of ordered microscopic structures were identified. The first one, namely, the spaghettilike one, is a structure in which the DNA strand is covered by a cylindrical lipid bilayer [18,20]. In the honeycomblike columnar inverted hexagonal phase, $H_\parallel^c$, the linear DNA molecules are surrounded by lipid monolayers forming inverted cylindrical micelles arranged on a hexagonal lattice [16]. Finally, a multilamellar structure has been reported consisting of alternating lipid bilayers and DNA monolayers [9,13–15,19]. This structure is formed in a self-assembled manner when mixing suspensions of CL with DNA. In addition to the enormous interest of these latter complexes as efficient delivery systems in gene therapy, their structure also found interest as the experimental realization of a system of weakly interacting quasi-two-dimensional (2D) smectic manifolds [21]. The nature and the extent of the DNA ordering in the 2D layers, confined between the lipid bilayers of the complex, have been quantitatively studied [15] and the possible equilibrium phases of stacked 2D smectic layers, dependent on the trans-

membrane lattice interactions, have been deeply investigated [17,22,23].

Metal ions may have considerable effects on the structure and conformational behavior of phospholipid bilayers. Phosphatidilcholine head groups behave as sensors of the electrostatic charge at the membrane surface [24]: for example, ions induce conformational changes in the polar head group region in the liquid-crystalline L_α phase [25,26], reorder the packing geometry of the saturated acyl chains in the ripple phase and enhance the appearance of the submain transition [27]. The interaction between Li^+ and the negatively charged head groups of phospholipids can lead to the formation of high-melting ion-lipid complexes [28], whereas Na^+ and K^+ only produce minor changes [29]. On the other hand, experimentally [30], as well as theoretically [31], it was shown that monovalent cations cannot condense DNA.

Within the general scope of studying new biological materials of potential interest for gene delivery systems, recently we have undertaken a systematic investigation of the interactions among neutral liposomes, DNA, and metal (Me) cations in triple L-DNA-Me^{n+} complexes [32]. These are expected to be more stable than binary neutral L-DNA complexes [33,34] and to exhibit lower cytotoxicity than the complexes with some kinds of CLs [35]. Evidence of the formation of L-DNA-Me^{2+} triple complexes was previously given by different techniques such as turbidimetry [36] and Fourier transform–infrared spectroscopy [37]. The stoichiometry and the stability constants of the complex with Mn^{2+} ions have been determined by comparing data of elemental analysis and electron spin resonance spectroscopy [36]. The structural characterization of these ternary complexes is essential in order to understand the role played by the metal cations in stabilizing the L-DNA interactions and therefore in the formation of supramolecular aggregates. Investigating the formation of L-DNA-Me^{2+} complexes should improve our understanding of how the genetically active material interacts with cells and hopefully will lead to improved transfection formulations. On the other hand, the correlation of gene carrier mechanism and transfection efficiency with the microscopic structure of the complex is a fascinating challenge for the near future. To this purpose, complexes of the neutral multilamellar liposome of dioleoyl phosphatidylcholine (DOPC) and DNA with different bivalent cations (Mn^{2+}, Co^{2+}, Fe^{2+}, Mg^{2+}) have been prepared and studied by means of synchrotron XRD. Even though evidence of the complex formation was found in all cases, we have primarily focused our structural analysis on the complex with Mn^{2+} because it gave the best signal-to-noise ratio at the solution concentrations used. Electron microscopy has been used too, as complementary technique, to gain further information on the structure and morphology of the complexes. The results reported clearly prove the formation of triple L-DNA-Me^{2+} complexes that self-assemble when mixing water suspensions of DOPC liposomes with DNA and metal ions. Based on the experimental data, a model is proposed for the structure of the complex, which consists of an ordered multilamellar structure with DNA sandwiched between the liposome bilayers and the Mn^{2+} ions acting as a bridge among the phosphate groups of DNA and the DOPC headgroups. These results show that Mn^{2+} ions have the potency to bind the negatively charged phosphate groups of phospholipids and suggest that neutral liposomes in the presence of bivalent metal ions behave as cationic liposomes.

II. EXPERIMENT

A. Materials

DOPC, DNA from calf thymus (base pairs=2675, contour length ≈ 0.9 μm) and metal ions Mn^{2+}, Mg^{2+}, Co^{2+}, Fe^{2+} as chloride were purchased from Fluka. Solutions of DNA, DOPC and metal ions were prepared in 4-(2-hydroxyl)piperazine-1-ethanesulphonic acid (HEPES) buffer (20 mM, pH=7.2). DOPC solutions were prepared evaporating appropriate volumes of DOPC chloroform solution in a stream of nitrogen and then vacuum desiccated for 2 h in order to remove traces of the solvent. Multilamellar vesicles (MLVs) were formed by hydrating the dry lipid in HEPES solution and vortexed several times during the 4 h hydration period. Appropriate aqueous concentrations of the three components have been used in the different experiments and their values are reported as specific experimental details. The concentration of DNA is reported as phosphate units. In all cases, the triple DOPC-DNA-Me^{2+} complexes were prepared by adding the metal ion solution to the DOPC-DNA solution.

B. XRD measurements and data analysis

Preliminary XRD measurements were carried out by means of an in-house diffractometer equipped with the Bruker AXS general area detector diffraction system. Monochromatized Cu $K\alpha$ radiation was used ($\lambda = 1.54$ Å). DOPC solutions of 60 mM concentration were used for the DOPC structure determination. Equal volumes of DOPC 60 mM, DNA 80 mM and metal ion 120 mM solutions were mixed and appropriate portions were used for the structure determination of the complex.

Simultaneous small- and wide-angle x-ray scattering (SAXS and WAXS) measurements were carried out using the 8-keV branch ($\lambda = 1.54$ Å) of the SAXS beamline at the synchrotron radiation source ELETTRA, Trieste, Italy [38]. The beam size was reduced to 0.5×3 mm^2 at the position of the sample, and the distance sample detector was set at 1.25 m. The sample was held in a 1-mm-diameter quartz glass capillary. Two one-dimensional position sensitive Gabriel-type delay-line detectors were used in order to cover simultaneously the SAXS and the WAXS regions. The q interval explored ($q = 4\pi \sin\theta/\lambda$, 2θ being the scattering angle) ranged between $q_{min} = 2.28 \times 10^{-3}$ Å^{-1} and $q_{max} = 2.10$ Å^{-1}. The resolution in the scattering plane was 2.8×10^{-3} Å^{-1} [full width at half maximum (FWHM)]. The calibration of the scattering angle scale was performed with silver-behenate powder for the SAXS and with *p*-bromobenzoic acid for the WAXS regime. Triple complexes DOPC-DNA-Me^{2+} were studied using different component ratios, obtained by mixing equal volumes of solutions of appropriate concentration of the free components previously prepared. In particular, the range of investigated ratios for the complex with Mn^{2+} is as follows: DOPC, 2 mM;

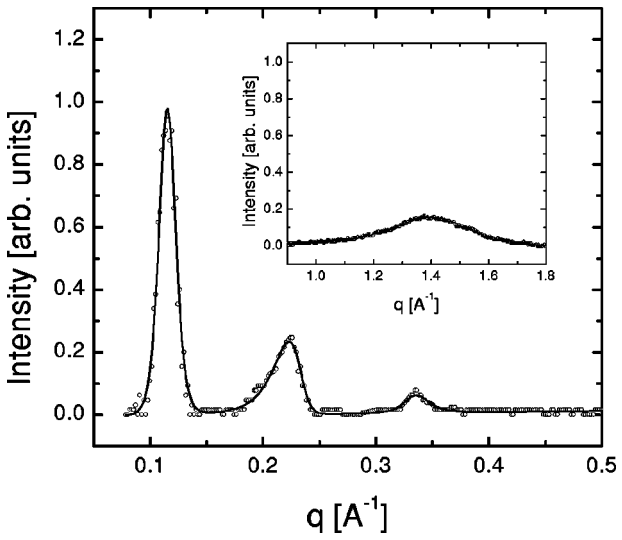

FIG. 1. XRD pattern of DOPC at 4.2% weight in HEPES solution. The inset shows the WAXS region of the spectrum. The measurement was carried out by means of the in-house diffractometer. The continuous lines are the best fit to the experimental data (○).

DNA, 2.67 mM; Mn^{2+}, 0.67–16 mM. Measurements were performed at room temperature after 2 min of incubation of the samples. In order to have good statistics, we chose an overall measuring time of 10 min. To avoid radiation damage of the samples, the overall 10-min spectra were obtained by summing five independent 2-min measurements, each taken on a fresh sample.

The raw scattering data were normalized against the incident-beam intensity using the signal of an ionization chamber mounted directly upstream of the sample. Patterns with empty sample holder and sample holder filled with HEPES solution were measured for background subtractions. The scattering data were further corrected for the detector efficiency. The best fit to the experimental profiles of the diffraction peaks were obtained by means of Split-Pearson VII lineshapes, with model parameter m (characterizing the tail-decay) variable between $m \approx 1$ (basic Lorentzian) and $m \approx 4$ (close to a modified Lorentzian).

The electron-density profile, $\Delta\rho$, along the normal to the bilayers, z, was calculated as a Fourier sum

$$\Delta\rho = \frac{\rho(z) - \langle\rho\rangle}{[\langle\rho^2(z)\rangle - \langle\rho\rangle^2]^{1/2}} = \sum_{l=1}^{N} F_l \cos\left(2\pi l \frac{z}{d}\right), \qquad (1)$$

where $\rho(z)$ is the electron density, $\langle\rho\rangle$ its average value, N is the highest order of the fundamental reflection observed in the XRD pattern, F_l is the form factor for the $(00l)$ reflection, d is the thickness of the repeating unit (including one lipid bilayer and one water layer), and the origin of the z axis is chosen in the middle of the lipid bilayer. The form factor F_l was calculated from the integrated intensity of the lth order peak I_l by means of Eq. (2),

$$I_l = s_l |F_l|^2 / q_l^2, \qquad (2)$$

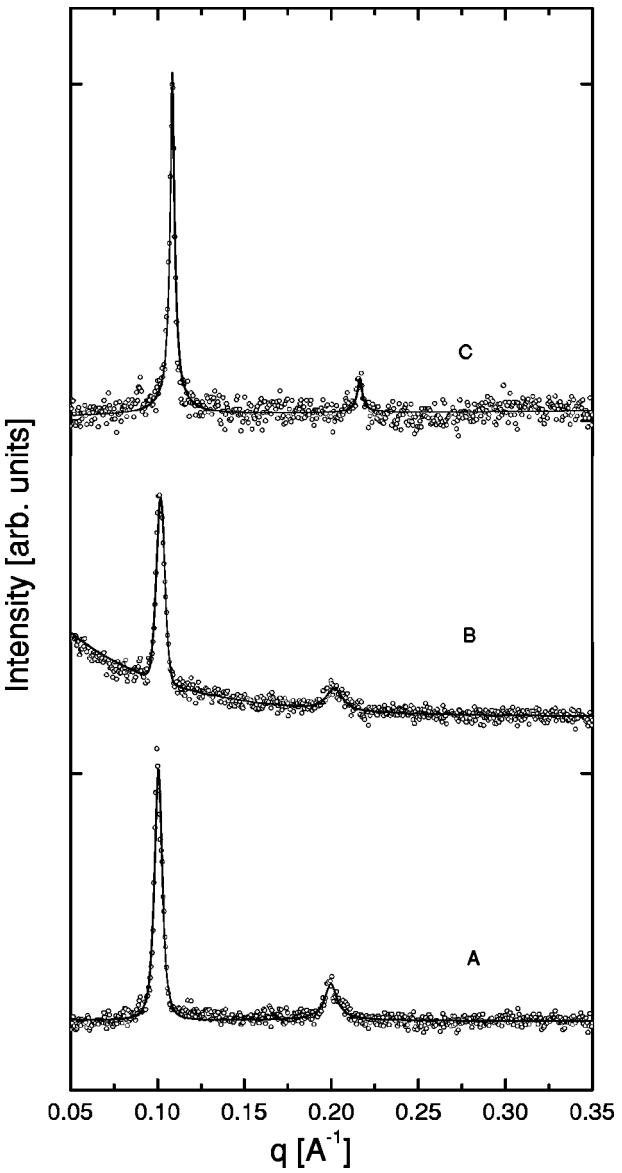

FIG. 2. Synchrotron XRD patterns of: (a) DOPC; (b) DOPC-DNA at 3:4 molar ratio; (c) DOPC-Mn^{2+} at 3:24 molar ratio. In all cases the DOPC weight in HEPES solution is 0.14%. The continuous lines are the best fit to the experimental data (○).

where $1/q_l^2$ is the usual Lorentz factor for unoriented samples ($q_l = 2\pi l/d$) and the additional correction factor s_l takes into account the effects of the liquid crystalline nature of the multilamellar structure according to the modified-Caillé theory [1,39]. Equation (2) determines the form factors except for the phase factor which must be ± 1 for symmetric bilayers. The phase problem was solved by means of a pattern recognition approach based on the histogram of the electron-density map [40], and the results were found to be in agreement with those obtained with different approaches [41,42].

C. Freeze-fracture electron microscopy

In the transmission electron microscopy measurements, a portion of DOPC 24-mM solution was used for the simple DOPC analysis, while samples of a mixture of equal vol-

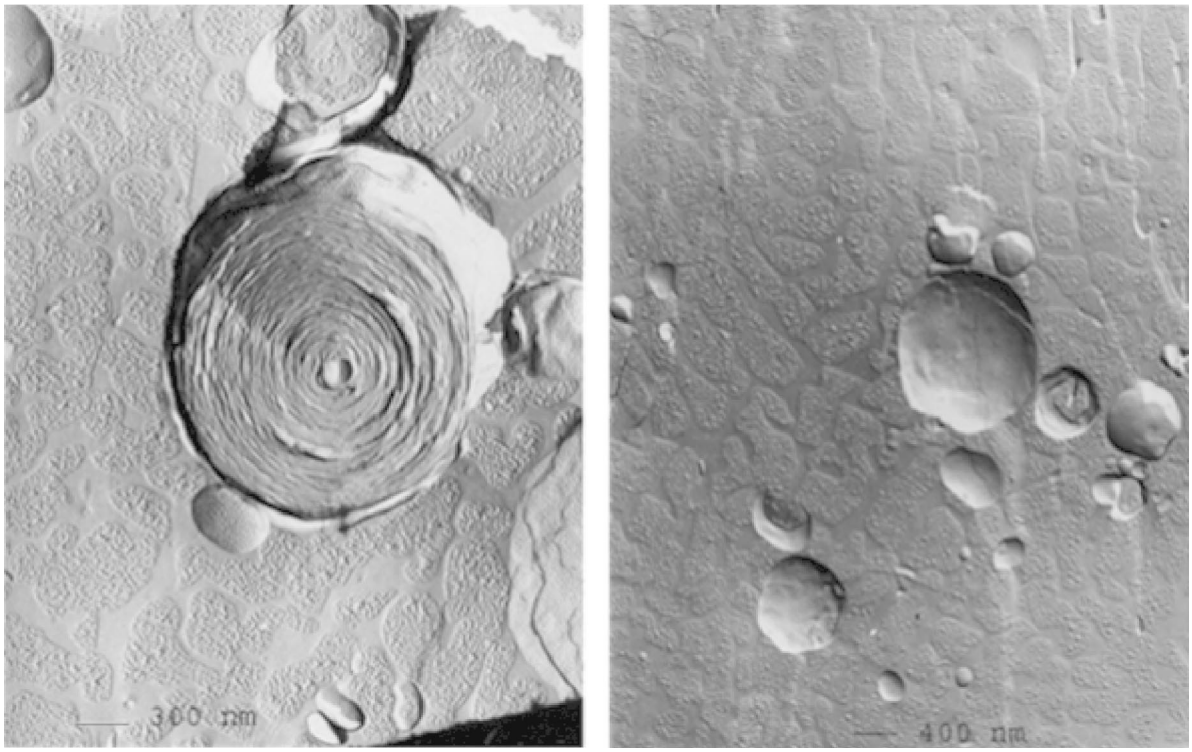

FIG. 3. Freeze-fracture EM micrographs of DOPC liposomes.

umes of DOPC 24 mM, DNA 32 mM and Mn^{2+} 48 mM, were prepared and used for the morphological analysis of the complex. To this mixture, 26% of glycerol was then added to increase the viscosity of the overall solution. The specimens were mounted on gold disks and frozen in freon 22 and liquid nitrogen, then fractured in Balzers BAF 301 device at a vacuum better than 7×10^{-5} Pa and at a temperature of 160 K. Immediately after fracture, the specimens were shadowed with platinum carbon at an angle of 45°. Replicas reinforced with carbon evaporation were then cleaned in chloroform-methanol blend and examined by a Philips CM 10 transmission electron microscope.

III. RESULTS AND DISCUSSION

Preliminary measurements were carried out on the multilamellar DOPC liposomes at different concentrations in buffered water solution, by means of the in-house diffractometer. Figure 1 shows the small-angle and wide-angle (inset) scattering of DOPC (4.2% weight) at room temperature, after subtraction for the sample holder and HEPES-solution background. The low-angle scattering consists of three fairly sharp peaks centered at $q_l=2\pi l/d$, with $d=56.4$ Å ($l=1,2,3$), corresponding to the first three orders of diffraction of the periodicity at $d=56.4$ Å, and is typical of the lamellar phases [43]. The WAXS region is featured by a wide diffuse peak centered about $d=2\pi/q=4.4$ Å, resulting from the liquidlike lateral (in-plane) packing of the melted hydrocarbon chains. This XRD pattern reveals the liquid-crystalline (LC) nature of the lamellar structure that corresponds to the well known L_α phase of DOPC [44,45]. A similar pattern was observed on reducing the DOPC weight in solution down to 0.14%. Due to extreme weakness of the scattered signal, the intensity of the diffracted peaks was very small at DOPC concentrations below 1% and the higher order peaks were hardly detectable. However, from the position of the first-order diffraction peak it was possible to measure a continuous increase of the lamellar d spacing from $d=56.4$ Å, at 4.2% DOPC weight, up to a maximum value $d=63.2$ Å, at 0.14%. This concentration corresponds to the L_α phase of DOPC in excess water [41,45]. In this condition, the swelling up of the uncharged lipid bilayers reaches its limiting hydration level and any excess water added to the sample is present as a bulk phase in the lipid dispersion, rather than being accommodated within the interbilayer space. Because of the control and the stability of the lamellar spacing, we chose the 0.14% as the reference DOPC weight concentration for the further measurements at the synchrotron source described in the following. On the other hand, this concentration is very close to the lipid concentrations used by other authors in the study of CL-DNA complex, which makes easier a comparison of the results.

Concerning the synchrotron XRD measurements, first we characterized the structural and morphological properties of the DOPC liposomes in our experimental conditions (0.14% weight). Figure 2(a) shows the small-angle scattering of DOPC at room temperature, after subtraction for the sample holder and HEPES-solution background. The XRD pattern corresponds to the L_α phase of DOPC with a lamellar repeat distance $d=63.2$ Å, in excellent agreement with the results of Ref. [41] for fully hydrated DOPC bilayers. The presence of only two orders of diffraction reflects the strong fluctuations of the bilayers. Freeze-fracture EM micrographs of

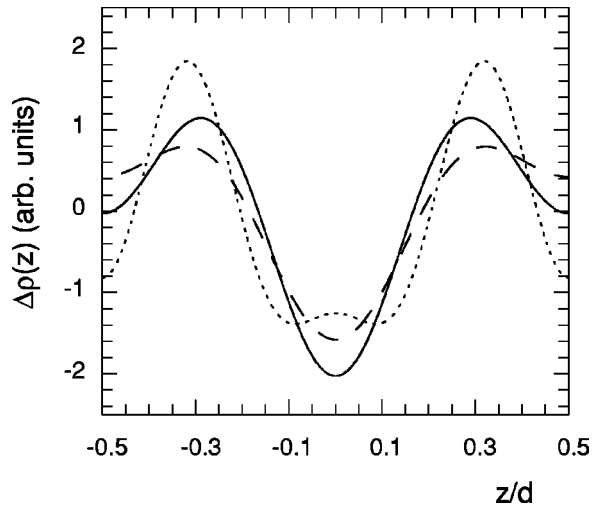

FIG. 4. Electron-density profile along the normal to the bilayers: the continuous line is for DOPC from data of Fig. 2(a), the dotted line is for DOPC from data of Fig. 1, and the dashed line is for DOPC-Mn^{2+} from data of Fig. 2(c).

DOPC (Fig. 3) show well-defined, mainly large, liposomes which are rather well separated from each other; typically heterogeneous particles in the size range 0.3–4.0 μm are observed. From the experimental FWHM of the first-order diffraction peak, after correction for the intrinsic spreading due to the instrumental resolution, we estimated a theoretical linewidth of $\Delta q = 2.2 \times 10^{-3}$ Å^{-1}. The average domain size D of the lamellar structure of the vesicles, calculated as $D \approx 2\pi/\Delta q = 2900$ Å, is consistent with the EM micrographs. Figure 4 (continuous line) shows the electron-density profile normal to the bilayers. The large central minimum corresponds to the region of the hydrocarbon tails whereas the two strong maxima correspond to the polar headgroups. The widths of the peaks are related to the extent of molecular disorder caused by fluctuations in the bilayer [46]. The distance between the electron-dense polar heads, measured as the distance between the centers of the electron-density peaks, gives a reliable estimate of the thickness, d_{HH}, of the lipid bilayer [47,48]. The value obtained is $d_{HH} = 37$ Å. From the lamellar spacing $d \cong 63$ Å and the value of d_{HH}, the interbilayer water thickness, d_W, was calculated as $d_W = d - d_{HH} = 26$ Å. In spite of the low resolution of the electron-density profile (due to the limited number of observable orders), these values are in excellent agreement with the structural data previously reported for fully hydrated DOPC bilayers [41]. The dotted line of Fig. 4 shows the electron-density profile of the DOPC liposome at 4.2% weight in buffered water solution, obtained from the XRD data of Fig. 1. A larger distance between the electron-density peaks accompanies the reduction of d ($d = 56.4$ Å), which results in a value of $d_{HH} = 36$ Å that remains essentially constant (within the experimental uncertainties). Besides d_{HH}, the bilayer thickness is also frequently represented as the Luzzati bilayer thickness $d_B = 2V_L/A$, where V_L is the volume of a single lipid molecule in the bilayer and A is the area per lipid measured parallel to the surface of the bilayer. The corresponding water spacing is then $d_W = d - d_B$. However, the values of d_B and d_W calculated in this way differ from the previous calculations for less than 1 Å [41]. As the bilayer-water interface is not as simple as a plane, a slightly more complex model [49] assumes that the headgroup has a length d_H over which it has a uniform area A'. This model allows for penetration of a number of water molecules in the volume $d_H(A - A')$ between the headgroups. From neutron diffraction data [50] the thickness of the headgroup may be estimated to be $d_H = 8$ Å. Then, a corresponding pure water distance

$$d_W = d - 2d_H - 2d_C \tag{3}$$

is defined, where $2d_C$ is the overall thickness of the hydrocarbon region. Using the structural data of Refs. [49,51,52] for the hydrocarbon-chain region, the value $d_C = 14.6$ Å is obtained, which gives the maximum bilayer thickness $d'_B = 2d_H + 2d_C = 45.2$ Å and the minimum water layer thickness [Eq. (3)] $d'_W = 18$ Å.

Addition of DNA to the DOPC solution did not produce any significant change in the structure of the vesicles, as shown by the XRD pattern of Fig. 2(b). Differently, addition of Mn^{2+} to the DOPC solution caused appreciable modifications of the structural arrangement of the lipid bilayers, as deduced from the SAXS pattern of Fig. 2(c). The shift of the diffraction peaks towards higher scattering angles corresponds to the reduction of the layer spacing to $d = 58.4$ Å, whereas the reduction of the FWHM of the peaks corresponds to the increase of the longitudinal correlation length. However, being the diffraction peaks resolution limited, it was possible only to estimate the lower limit of the domain size, i.e., $D \geqslant 2900$ Å. The significant change of the second-to-first-order integrated intensity ratio revealed a structural modification of the molecular packing within the layers. The dashed line of Fig. 4 shows the electron-density profile in the DOPC-Mn^{2+} solution deduced from the XRD data of Fig. 2(c). All these effects are indicative of a strong influence of the metal ions on the lamellar structure of the liposomes. In neutral liposomes, the equilibrium interbilayer distance results from a critical balance between the attractive van der Waals interaction and the repulsive hydration force [53] originating from interactions between the hydrated phosphate groups of the polar heads. Various direct measurements of the hydration force have shown that the repulsive hydration pressure P decays exponentially with the amount of the interbilayer water (or, equivalently, with the interbilayer distance) [45,53–58].

$$P = P_0 \exp(-n_W/\nu) = P_0 \exp(-d'_W/\lambda), \tag{4}$$

where n_W is the number of water molecules per lipid, d'_W is the water interbilayer thickness, P_0 is the nominal pressure at zero hydration, ν represents the hydration force decay constant in units of water molecules and λ is the space decay length. Choosing for ν the average of the values available in the literature [45,53,58], i.e., $\nu = 3.65$, and taking $\lambda = 2.2$ Å [41], we find that the experimental value $d'_W = 18$ Å corresponds to $n_W \approx 30$, in agreement with the value expected for fully hydrated DOPC [41,45]. The attractive interaction of

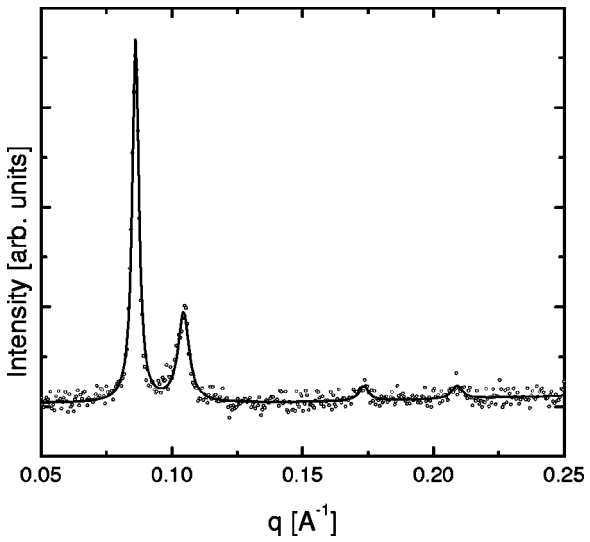

FIG. 5. Synchrotron XRD pattern of DOPC-DNA-Mn^{2+} at 3:4:12 molar ratio. The continuous line is the best fit to the experimental data (○).

the metal ions with the polar heads of DOPC leads to partial dehydration of the headgroups. A new equilibrium characterized by a shorter interbilayer distance is reached, where the stronger attractive action promoted by the metal cations is balanced by an equivalent stronger repulsive hydration force. In addition, the presence of metal cations favors a better packing of the multilayered structure, which results in an increase of the positional correlation length evidenced by the reduction of the peak width. Finally, the metal ions in the region close to the polar heads increase slightly the electron density in the water layer as evidenced by the electron-density profile shown by the dotted line of Fig. 4. From this figure, a thickness $d_{HH} \cong 37$ Å of the lipid bilayer has been estimated, which confirms that the reduction of periodicity d of the multilamellar structure is due to reduction of the water layer thickness. In particular, the Luzzati water thickness becomes $d_W = d - d_{HH} = 21$ Å and $d'_W = d - d'_B = d - (2d_H + 2d_C) = 13$ Å. According to Eq. (4), the change of d'_W from 18 to 13 allows one to estimate a reduction in n_W of about 27% when metal ions are added to the solution.

XRD measurements of the DOPC-DNA-Mn^{2+} complex were carried out for a wide range of molar ratios of the components. Figure 5 shows the SAXS spectrum of DOPC-DNA-Mn^{2+} at 3:4:12 molar ratio. This pattern is characterized by two intense sharp peaks at $d_1 = 73.4$ Å and $d_2 = 60.4$ Å with the corresponding first-order harmonics at 36.7 Å and 30.2 Å, respectively. The WAXS pattern (not shown in the figure) exhibits only a wide diffuse peak centered about $q \approx 1.43$ Å^{-1}, very similar to that observed for DOPC in solution, which excludes crystalline order and reflects the short-range liquidlike positional ordering of the lipids within the layers, with an average distance $\approx 2\pi/q = 4.4$ Å. A similar pattern was observed for all the samples investigated, that ranged from 3:4:1 to 3:4:24 molar ratios. The relevant XRD data of these spectra are summarized in Table I as a function of the relative concentration of metal ions (with a fixed DOPC/DNA ratio). These data show a

TABLE I. The lamellar repeat distance of the L_α^c phase of the triple complex (d_1) and the L_α phase of DOPC (d_2) as a function of the metal ion concentration.

DOPC	DNA	Mn^{2+}	d_1 (Å)	d_2 (Å)
3	4	1		63.8
3	4	3	73.4	62.6
3	4	4	73.3	63.3
3	4	6	73.4	62.4
3	4	9	73.5	61.0
3	4	12	73.4	60.4
3	4	18	73.5	60.0
3	4	24	73.1	58.8

substantial constancy of the d_1 spacing accompanied by an appreciable continuous decrease of d_2 from 63.8 Å (3:4:1) to 58.8 Å (3:4:24). For the reasons discussed below, it is important to observe that the value $d_2 = 58.8$ Å corresponding to 3:4:24 is very close to the value of the layer spacing measured in the DOPC-Mn^{2+} (3:24) mixture, i.e., $d = 58.4$ Å.

The above XRD data are indicative of the coexistence of two distinct LC multilamellar structures with incommensurate periodicities: the d_2 spacing can be associated with the L_α phase of the DOPC whereas the higher spacing d_1 reflects the presence of the L_α^c lamellar phase of the triple DOPC-DNA-Mn^{2+} complex (this phase is one of the condensed lipid-polyelectrolyte phases, for which the lipid phase nomenclature plus an additional "*c*" for "condensed" or "complex" is used [16]). This latter consists of a structure similar to that found in CL-DNA complexes [10,13], which is made of stacks of alternating lipid bilayers and DNA monolayers. A schematic picture of the local structural arrangement of the triple complex in the L_α^c phase is shown in Fig. 6 whereas the electron-density profile within the repeating unit of the complex is shown in Fig. 7 (the structure

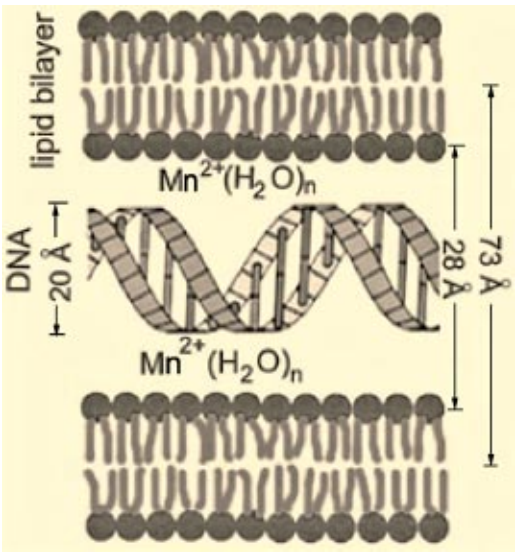

FIG. 6. Schematic picture of the structure of the L_α^c phase of the triple complex DOPC-DNA-Mn^{2+}.

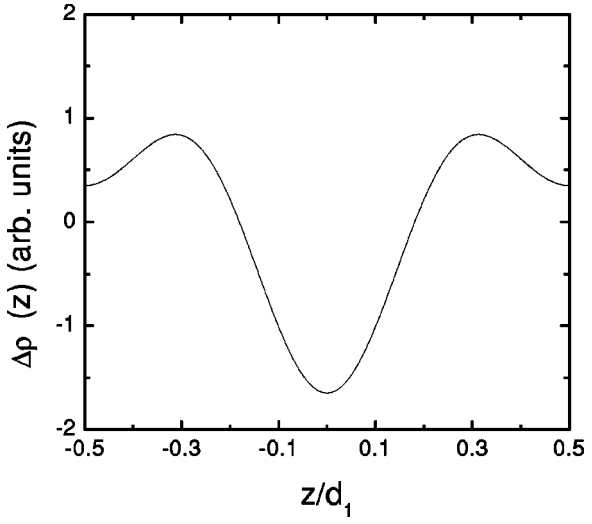

FIG. 7. Electron-density profile along the normal to the bilayers in the L_α^c phase of the triple complex DOPC-DNA-Mn^{2+} at 3:4:12 molar ratio.

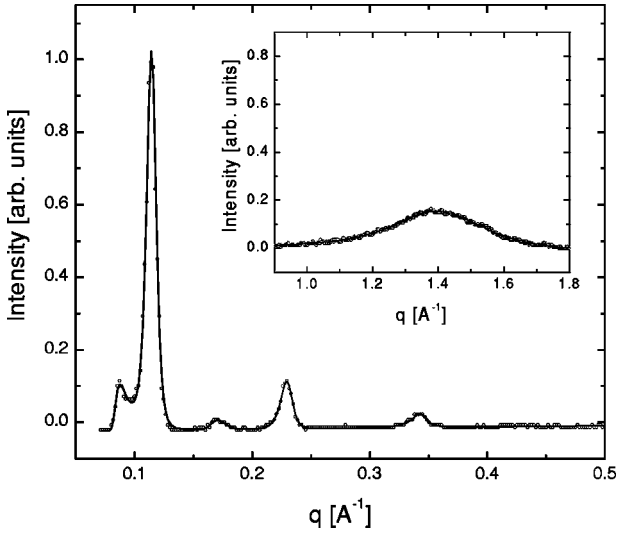

FIG. 8. XRD pattern of the triple complex DOPC-DNA-Mn^{2+} (3:4:12) at 4.2% DOPC weight in HEPES solution. The inset shows the WAXS region of the pattern. The measurement was carried out by means of the in-house diffractometer. The continuous lines are the best fit to the experimental data (○).

factors are $F_1=-1.000$ and $F_2=-0.648$). The DNA strands are sandwiched between the lipid bilayers and are bound to these through the metal ions. The overall thickness of the lipid bilayer, estimated from the position of the two maxima in Fig. 6, is $d_B \approx 45$ Å which is very close to that found in pure DOPC. The corresponding interbilayer thickness $d-d_B \approx 28$ Å is then sufficient to accommodate one hydrated (one-water) shell DNA helix of 25 Å [59] plus two thin layers of metal cations (≈ 3 Å).

A similar behavior was observed for different total concentrations of the DOPC-DNA-Mn^{2+} mixture in buffered water (at the same relative concentration of the components). As an example, Fig. 8 shows the SAXS and WAXS XRD pattern of the DOPC-DNA-Mn^{2+} mixture (3:4:12) at 4.2% concentration of DOPC in buffered water. Two sets of peaks are identified: the first one corresponds to the fundamental and the first two harmonics of the reflection at $d_1=71.5$ Å, associated with the L_α^c phase of the triple complex; the second one corresponds to the fundamental and the first har-

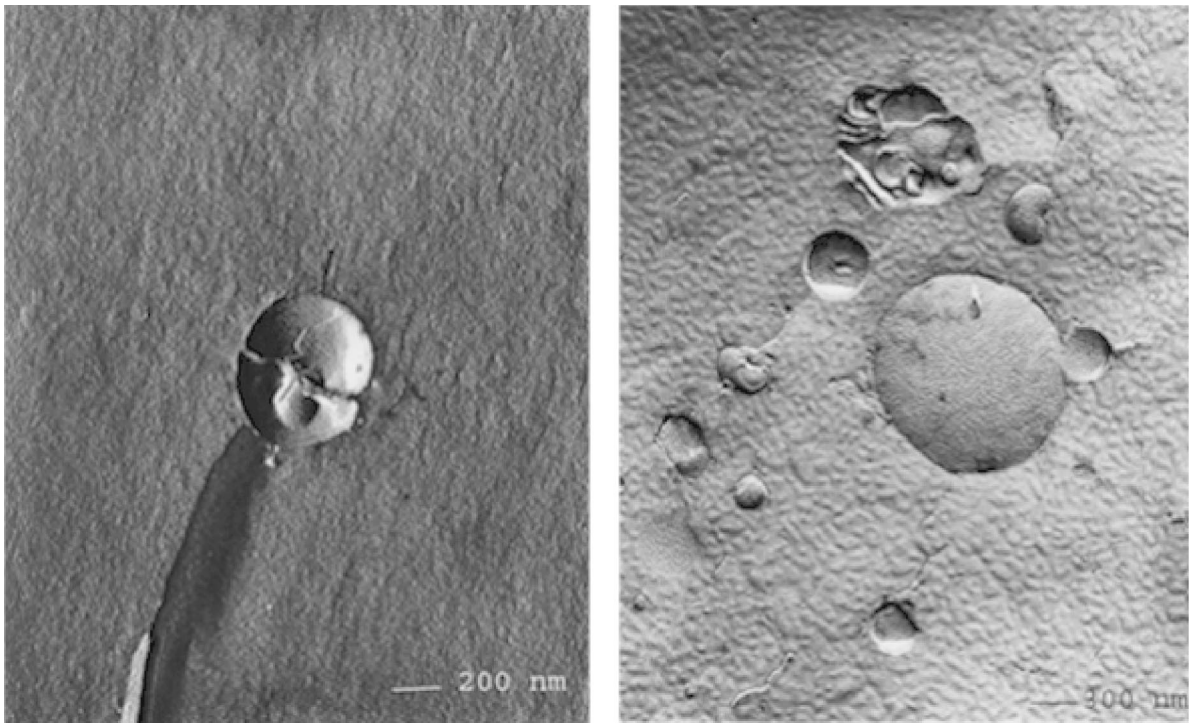

FIG. 9. Freeze-fracture EM micrographs of the DOPC-DNA-Mn^{2+} mixture at 3:4:6 molar ratio.

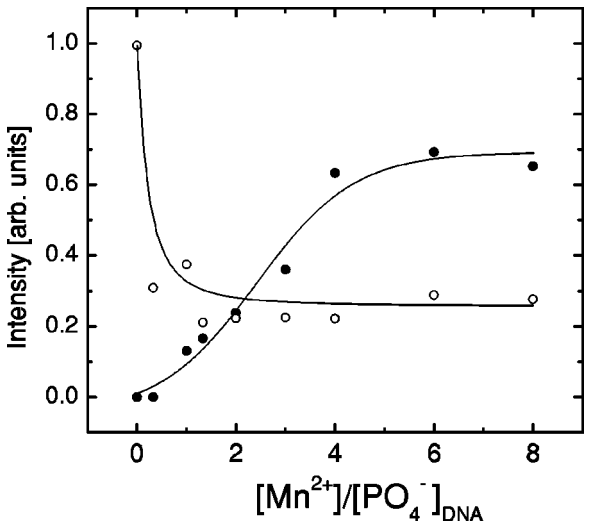

FIG. 10. The integrated intensities of the first-order diffraction peak of the triple complex (●) and the DOPC liposome (○), as a function of the ratio of the metal ion concentration to the concentration of the DNA phosphate groups. The continuous lines are guides for the eyes.

monic of the reflection at $d_2 = 55.1$ Å, associated with the L_α phase of DOPC.

From the above XRD data, it must be concluded that the formation of the triple complex is promoted by the positively charged metal ions that bind the polar heads of DOPC with the negatively charged phosphate groups of DNA. This experimental evidence suggests that neutral liposomes in the presence of metal ions behave similarly to CLs. In fact, in both cases, the driving force for complex condensation is the release of counterions. DNA carries 20 phosphate groups per helical pitch of 34.1 Å, and due to Manning condensation, 76% of these anionic groups are permanently neutralized by their counterions, which lead to a distance between anionic groups of the order of the Bjerrum length (7.1 Å) [60]. In the triple-complex condensation, the Mn^{2+} ions play the same role as the cationic head of the lipid in that they tend to fully neutralize the phosphate groups of the DNA, thus replacing and releasing in the solution the original counterions.

The simultaneous presence of the two multilamellar structures requires a model to explain such coexistence. To this purpose, the XRD data were complemented with morphological cryo-EM data of the triple complexes and the results were compared with those obtained in CL-DNA complexes. Figure 9 shows representative EM micrographs of the DOPC-DNA-Mn^{2+} mixture. In the range of molar ratios investigated we always observed single spheroidal or distinct semifused aggregates of a few (mainly two) globules with an average size between ≈ 200 nm and ≈ 900 nm, similar to those observed in CL-DNA complexes after comparable incubation time [18]. The surface of the globules is smooth as it is typical of LC phases. We have interpreted these aggregates as being constituted by distinct LC multilamellar structures: a given fraction of the total number of globules consists of the L_α^c phase of the triple complex, whereas the rest of the globules persist as the L_α phase of DOPC. In our

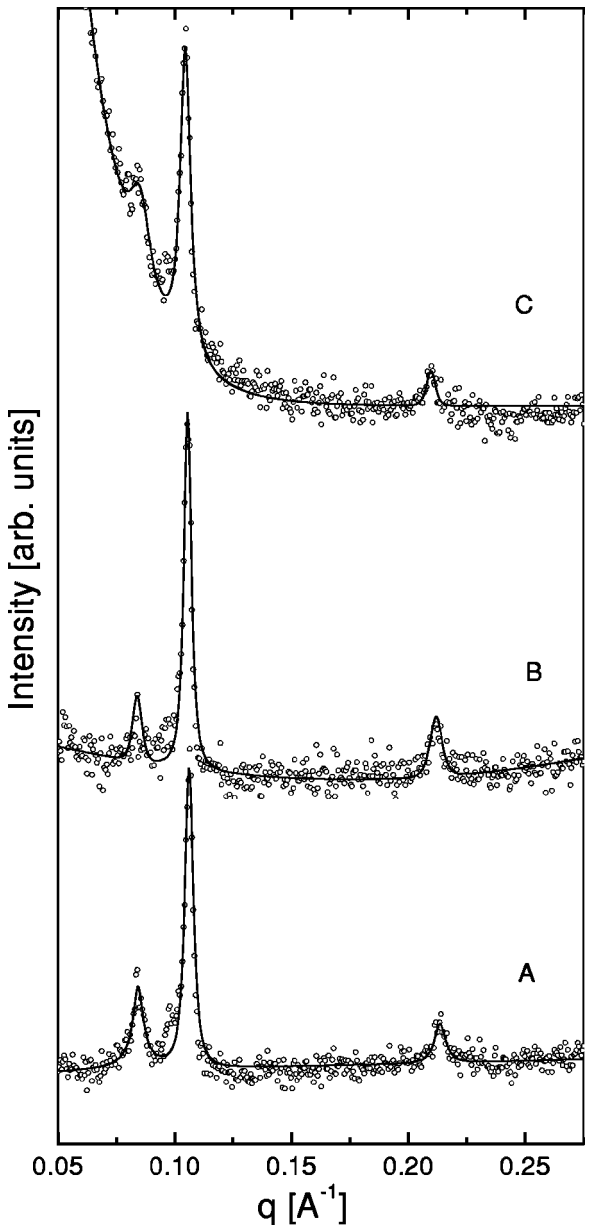

FIG. 11. Synchrotron XRD pattern of DOPC-DNA-Me^{2+} triple complexes at 3:4:24 molar ratio: (a) Me=Co^{2+}, (b) Me=Mg^{2+}, (c) Me=Fe^{2+}. The continuous lines are the best fit to the experimental data (○). In each of the pattern, the peak at lower q is due to the L_α^c phase of the complex while the remaining two (fundamental and first harmonic) are due to the L_α phase of the DOPC.

picture of the triple-complex formation, the linear DNA molecules are condensed in the mixture with the starting MLV liposomes, whereby both lipid and DNA undergo a complete topological transformation into compact spheroidal particles within which the complexes have ordered structure. This process should be similar to that observed in CL-DNA self-assembled complexes [13] apart from the different fusogenic agent and the different nature of the starting liposomes (multilamellar vesicles instead of unilamellar vesicles). This latter, however, is a relevant difference because it involves a more complex phenomenology of the triple-complex formation process. In the case of CLs, the original samples did not

consist of multilamellar vesicles prior to the addition of DNA. It is therefore clear that the transition from unilamellar to multilamellar structure is induced by the complexation of DNA with the small cationic unilamellar vesicles. The DNA adsorbs between the liposome bilayers giving rise to an alternating, locally flat lamellar structure; in this process, the DNA intercalates between the bilayers forming a more or less ordered array of chains. Spheroidal macroaggregates are then formed, composed of flat lipid bilayers with DNA packed between them in a sandwichlike structure. These multilamellar aggregates were identified in several lipid systems and at various DNA to lipid ratios, by means of scattering [10,13] and cryo-EM experiments [19]. In our case, MLVs of the liposome are contained in the original sample and therefore the lipid bilayer-DNA aggregation involved in the complex formation requires a simultaneous breaking up of the multilamellar liposomes, starting from the external layers of the vesicles. In other words, while the condensation between lipid bilayers and solution DNA proceeds, promoted by the fusogenic action of the metal ions, the original self-closed vesicle structure of curved bilayers must continuously open to provide the lipid material for self-assembling of the triple complex. This process involves the external layer of the vesicle and produces a continuous reduction of the original vesicle volume until a minimum size is reached. When the steady state is reached, globules of the multilamellar structured triple complex coexist with the rest of the original MLVs characterized by a reduced average size. This model of lipid vesicle disaggregation and reaggregation into a different multilamellar structure is supported by the cryo-EM data of the triple complexes that always showed particles with an average size much smaller than that of the original vesicles (Fig. 9). Basing solely on the present data, only a qualitative explanation of this mechanism can be proposed. The driving force for DNA complexation with lipids is due to the release of counterion entropy upon complexation [61,62], the energy involved being very high (of order 1 $kT/$Å). Accordingly, we expect that DNA will find energetically more favorable to form some sort of complex with lipids and metal ions. On the other hand, from calculations of minimum free energy of the aggregated lipids (including head-head and tail-tail interaction energy and the interfacial energy), it has been shown [20] that the locally flat lamellar structure of the complex should be the most stable compared with other possible geometries such as those of ''bead on string'' or ''cylindrical'' complexes, regardless of the lipid properties. Therefore, the aggregation process gives rise to a multilamellar locally flat structure of the complex. However, a further contribution to the total free energy of the sample should come from the organization of these lamellar domains within the globular microaggregates. This contribution increases with their dimension and, beyond a given size, further growth of the complex becomes energetically unfavorable. The relative concentration of the two multilamellar species at equilibrium is expected to depend on several physical and chemical parameters such as water dilution of the lipids, average size of the vesicles, temperature and molar ratios of the components of the mixture. The latter dependence is confirmed by further analysis of the XRD data. The integrated intensity of each of the two first-order diffraction peaks in the SAXS region is proportional to the volume fraction of the sample that is occupied by the corresponding multilamellar structure. Figure 10 shows the integrated intensities of the peak at d_1 (from the triple complex, full circles) and at d_2 (from DOPC, open circles) versus the ratio of the metal ion concentration to the one of the DNA phosphate groups. The data demonstrate that an increase of the metal ion concentration favors the formation of the triple complex: the increase of the complex volume fraction is accompanied by a complementary reduction of the amount of DOPC liposomes until a saturation is reached (above $[Mn^{2+}]/[PO_4^{2-}] \approx 4$) corresponding to constant volume fractions of the two structures ($\approx 70\%$ and 30%, respectively).

XRD measurements were also systematically carried out on triple mixtures of the DOPC, DNA, and Mn^{2+} components at different DOPC/DNA molar ratios. All these measurements evidenced the formation of the triple complex and its coexistence at equilibrium with the DOPC MLVs. However, an analysis of the effects of the relative concentration of the three components on the formation and the equilibrium concentration of the L_α^c phase is beyond purpose of the present paper and will be reported elsewhere.

Differently from what was found in CL-DNA complexes, in our experimental conditions the DOPC-DNA-Mn^{2+} complex did not exhibit two-dimensional ordering or regularity of the DNA packing within the lipid bilayers. In fact, the XRD data of CL-DNA complexes [14,15] evidenced, apart from the sharp lamellar peaks, a much broader and weaker peak arising from the DNA-DNA correlations. The position of this was strongly dependent on the neutral-to-cationic lipid ratio, shifting over a wide range corresponding to a change in the DNA interhelical spacing from $d \approx 26$ Å (close packed) to $d \approx 55$ Å (significant dilution). In our case, the absence of this peak can be justified considering that the higher mobility of the fusogenic agent, i.e., the metal ions, does not induce enough constraint to allow the DNA chains to assume a regular packing within the lipid bilayers. On the other hand, measurements performed up to 30 min after the sample preparation did not show any change of the XRD pattern, thus excluding possible effect of the incubation time in removing the DNA positional disorder that is naturally involved in the condensation process. In addition, the XRD data on similar complexes obtained with different cations such as Co^{2+}, Fe^{2+}, Mg^{2+} (Fig. 11), while showing the formation of analogous self-assembled multilamellar structures, confirmed at the same time the lack of DNA-DNA positional correlations.

IV. CONCLUSIONS

We have studied the structure and the morphology of the DOPC-DNA-Mn^{2+} complex that is formed in a self-assembled manner when liposome, DNA and bivalent metal ions are mixed in solution. The complex is characterized by the lamellar symmetry of the L_α^c phase and is rather heterogeneous with respect to size and shape. The structure of the complex consists of an ordered multilamellar assembly where the hydrated DNA helices are sandwiched between the

liposome bilayers. The condensation of the DNA in the complex is induced by the metal cations that bind the lipid polar heads with the negatively charged phosphate groups of DNA. This represents a striking example of supramolecular chemistry.

Further experiments with higher resolution and complementary techniques are needed to elucidate the nature of the intermolecular forces and the interplay between repulsive hydration forces and attractive electric interactions. Future studies may also reveal regimes with in-layer correlations between the DNA chains as well as correlation from layer to layer, in analogy to CL-DNA complexes and recent theoretical findings in highly condensed DNA phases. To test how promising these complexes are as synthetically based nonviral carriers of DNA vectors for gene therapy, we have planned specific experiments to measure the transfection efficiency and to determine the structural parameters relevant to it. These should favor our understanding of the interactions of the complex with cellular lipids and the mechanism of DNA transfer across the nuclear membrane.

ACKNOWLEDGMENTS

It is a pleasure to thank Dr. D.E. Lucchetta, R. Marzocchini, C. Conti, and Dr. F. Cingolani for participation in the XRD experiments and assistance in the sample preparation. We acknowledge useful discussions with Professor G. Principato.

[1] R. Zhang, R.M. Suter, and J.F. Nagle, Phys. Rev. E **50**, 5047 (1994), and references therein.
[2] R.H. Austin, J.P. Brody, E.C. Cox, T. Dike, and W. Volkmuth, Phys. Today **50** (2), 32 (1997).
[3] D. D. Lasic, *Liposomes: from Physics to Applications* (Elsevier, Amsterdam, 1993).
[4] V.G. Budker, Y.A. Kazachkov, and L.P. Naumova, FEBS Lett. **95**, 143 (1978).
[5] B. Budker, A.A. Godovikov, L. Naumova, and I.A. Slepneva, Nucleic Acids Res. **8**, 2499 (1980).
[6] B. Brosius and D.J. Riesner, J. Biomol. Struct. Dyn. **4**, 271 (1986).
[7] P.L. Felgner, T.R. Gradek, M. Holm, R. Roman, H.W. Chan, M. Venz, J.P. Northrop, G.M. Ringold, and M. Danielson, Proc. Natl. Acad. Sci. U.S.A. **84**, 7413 (1987).
[8] H.E.J. Hofland, L. Shephard, and S.M. Sullivan, Proc. Natl. Acad. Sci. U.S.A. **93**, 7305 (1996).
[9] M.S. Spector and J.M. Schnur, Science **275**, 7 (1997).
[10] D.D. Lasic, H. Strey, M.C.A. Stuart, R. Podgornik, and P.M. Frederick, J. Am. Chem. Soc. **119**, 832 (1997).
[11] R.G. Crystal, Science **270**, 404 (1995); R.C. Mulligan, *ibid.* **260**, 926 (1993).
[12] J.G. Smith, R.L. Walsem, and J.B. German, Biochim. Biophys. Acta **1154**, 327 (1993).
[13] J.O. Rädler, I. Koltover, T. Salditt, and C.R. Safinya, Science **275**, 810 (1997).
[14] T. Salditt, I. Koltover, J.O. Rädler, and C.R. Safinya, Phys. Rev. Lett. **79**, 2582 (1997).
[15] T. Salditt, I. Koltover, J.O. Rädler, and C.R. Safinya, Phys. Rev. E **58**, 889 (1998).
[16] I. Koltover, T. Salditt, J.O. Rädler, and C.R. Safinya, Science **281**, 78 (1998).
[17] F. Artzner, R. Zantl, G. Rapp, and J.O. Rädler, Phys. Rev. Lett. **81**, 5015 (1998).
[18] B. Sternberg, F.L. Sorgi, and L. Huang, FEBS Lett. **356**, 361 (1994).
[19] B.J. Battersby, R. Grimm, S. Huebner, and G. Cevc, Biochim. Biophys. Acta **1372**, 379 (1998).
[20] N. Dan, Biochim. Biophys. Acta **1369**, 34 (1998).
[21] C.S. O'Hern and T.C. Lubensky, Phys. Rev. Lett. **80**, 4345 (1998).
[22] L. Golubović and M. Golubović, Phys. Rev. Lett. **80**, 4341 (1998).
[23] L. Golubović, T.C. Lubensky, and C.S. O'Hern, Phys. Rev. E **62**, 1069 (2000).
[24] J. Seelig, P.M. Macdonald, and P.G. Scherrer, Biochemistry **26**, 7535 (1987).
[25] M.F. Brown and J. Seelig, Nature (London) **269**, 721 (1977).
[26] H. Akutsu and T. Nagamori, Biochemistry **30**, 4510 (1991).
[27] K. Pressl, K. Jørgensen, and P. Laggner, Biochim.Biophys. Acta, Biochim. Biophys. Acta **1325**, 1 (1997).
[28] J. Mattai, H. Hauser, R.A. Demel, and G.G. Shipley, Biochemistry **28**, 2322 (1989).
[29] H. Hauser and G.G. Shipley, Biochim. Biophys. Acta **813**, 343 (1985).
[30] V.A. Bloomfield, Biopolymers **31**, 1471 (1991).
[31] G.Q. Manning, Q. Rev. Biophys. **11**, 179 (1978).
[32] P. Bruni, F. Cingolani, O. Francescangeli, M. Iacussi, and G. Tosi, in *Proceedings of the 15th IUPAC Conference on Physical Organic Chemistry, Goteborg, 2000* (Stadsbyggnadskontoret, Goteborg, 2000), Book of Abstracts, p. 12.
[33] A. Koiv, J. Palvimo, and P.K.J. Kinnunen, Biochemistry **34**, 8018 (1995).
[34] B.B. Fedorov, P.N. D'yachkov, and R.J. Zhdanov, Russ. Chem. Bull. **48**, 2046 (1999).
[35] P. Pinnaduwage and L. Huang, Biochemistry **31**, 2850 (1992).
[36] P. Bruni, G. Gobbi, G. Morganti, M. Iacussi, E. Maurelli, and G. Tosi, Gazz. Chim. Ital. **127**, 513 (1997).
[37] P. Bruni, F. Cingolani, M. Iacussi, F. Pierfederici, and G. Tosi, J. Mol. Struct. **565-566**, 237 (2001).
[38] H. Amenitsch, S. Bernstorff, M. Kriechbaum, D. Lombardo, H. Mio, M. Rappolt, and P. Laggner, J. Appl. Crystallogr. **30**, 872 (1997).
[39] R. Zhang, S. Tristram-Nagle, W. Sun, R.L. Headrick, T.C. Irving, R.M. Suter, and J.F. Nagle, Biophys. J. **70**, 349 (1996).
[40] O. Francescangeli, D. Rinaldi, M. Laus, G. Galli, and B. Gallot, J. Phys. II **6**, 77 (1996), and references therein.
[41] S. Tristram-Nagle, H.I. Petrache, and J.F. Nagle, Biophys. J. **75**, 917 (1998).
[42] C.R. Worthington and H.I. Khare, Biophys. J. **23**, 407 (1978).
[43] V. Luzzati, in *Biological Membranes*, edited by D. Chapman

and F. H. Wallah (Academic Press, New York, London, 1968), pp. 21–123.
[44] R. Koynova and M. Caffrey, Biochim. Biophys. Acta **1376**, 91 (1998).
[45] A.S. Ulrich, M. Sami, and A. Watts, Biochim. Biophys. Acta **1191**, 225 (1994), and references therein.
[46] M.C. Wiener and S.H. White, Biophys. J. **59**, 162 (1991).
[47] P.B. Hitchcock, R. Mason, K.M. Thomas, and G.G. Shipley, Proc. Natl. Acad. Sci. U.S.A. **71**, 3036 (1974).
[48] T.J. McIntosh and S.A. Simon, Biochemistry **25**, 4058 (1986).
[49] J.F. Nagle and M.C. Wiener, Biochim. Biophys. Acta **942**, 1 (1988).
[50] G. Buldt, H.U. Gally, J. Seelig, and G. Zaccai, J. Mol. Biol. **134**, 673 (1979).
[51] J.F. Nagle, R. Zhang, S. Tristram-Nagle, W. Sun, H.I. Petrache, and R.M. Suter, Biophys. J. **70**, 1419 (1996).
[52] J. Lemmich, K. Mortensen, J.H. Ipsen, T. Hønger, R. Bauer, and O.G. Mouritsen, Phys. Rev. E **53**, 5169 (1996).
[53] P.R. Rand and V.A. Parsegian, Biochim. Biophys. Acta **988**, 351 (1989).
[54] G. Bryant and J. Wolf, Cryolett. **14**, 23 (1992).
[55] G. Cevc and D. Marsh, Biophys. J. **47**, 21 (1985).
[56] J.N. Israelachvili and H. Wennerström, J. Phys. Chem. **96**, 520 (1992).
[57] D.M. LeNeveu, R.P. Rand, and V.A. Parsegian, Nature (London) **259**, 601 (1976).
[58] D. Marsh, Biophys. J. **55**, 1093 (1989).
[59] R. Podgornik, D.C. Rau, and W.A. Parsegian, Macromolecules **22**, 1780 (1989).
[60] G.S. Manning, J. Chem. Phys. **51**, 924 (1969).
[61] I. Koltover, T. Salditt, and C.R. Safinya, Biophys. J. **77**, 915 (1999).
[62] N. Dan, Biophys. J. **71**, 1267 (1996).